Numerical and Experimental Study on Metal Organic Vapor-Phase Epitaxy of InGaN/GaN Multi-Quantum-Wells

Changsung Sean Kim
Jongpa Hong
Jihye Shim
Bum Joon Kim
Hak-Hwan Kim
Sang Duk Yoo
Won Shin Lee

Corporate R&D Institute CAE Group,
SAMSUNG Electro-Mechanics Co. Ltd.,
Suwon, Gyunggi-Do 443-743, Korea

A numerical and experimental study has been performed to characterize the metal organic vapor-phase epitaxy (MOVPE) growth of InGaN/GaN multi-quantum-wells. One of the major objectives of the present study is to predict the optimal operating conditions that would be suitable for the fabrication of GaN-based light-emitting diodes using three different reactors, vertical, horizontal, and planetary. Computational fluid dynamics (CFD) simulations considering gas-phase chemical reactions and surface chemistry were carried out and compared with experimental measurements. Through a lot of CFD simulations, the database for the multiparametric dependency of indium incorporation and growth rate in InGaN/GaN layers has been established in a wide range of growth conditions. Also, a heating system using radio frequency power was verified to obtain the uniform temperature distribution by simulating the electromagnetic field as well as gas flow fields. The present multidisciplinary approach has been applied to the development of a novel-concept MOVPE system as well as performance enhancement of existing commercial reactors. [DOI: 10.1115/1.2956513]

Keywords: metal organic vapor-phase epitaxy, InGaN, multi-quantum-well, light-emitting diode, surface chemistry, radio frequency power, electromagnetic field

Introduction

Light-emitting diodes (LEDs) have recently attracted more attention as a potential alternative of incandescent bulbs and fluorescent lamps, expecting an emerging market of general lighting. LEDs have promising advantages over existing electric light bulbs. It has been noted that the typical life span of LEDs is about 10 years, twice as long as fluorescent lamps and approximately 20 times longer than the incandescent bulbs. LEDs generate much less thermal energy than incandescent bulbs with the same light output. LEDs are also free of environmental pollutants such as neon, helium, and argon discharged from fluorescent lamps. Lighting modules with combination of red, green, and blue LEDs can emit light of an intended color without additional color filters that traditional lighting methods adopt.

One of most popular white LED technologies is the use of a GaN-based blue LED and an yttrium aluminum garnet (YAG) phosphor because of its noticeable characteristics of small size, light weight, and easy operation [1]. As an alternative approach, we have investigated the combination of discrete red, green, and blue LEDs in order to realize a high efficacy white LED. Compared to red and blue LEDs, green LED still leaves much more room for improvement in luminescent efficacy. The production of green LEDs by metal organic vapor-phase epitaxy (MOVPE) is closely related to the ability to grow InGaN/GaN multi-quantum-wells (MQWs) with high indium compositions. A conventional MOVPE process of Group-III-nitride compounds in a simple reactor is illustrated in Fig. 1. At inlet, Group-III precursors and ammonia as Group-V precursor are introduced into the reactor to build up the epitaxial layers including the InGaN/GaN MQWs, as depicted in Fig. 2. Typically, the thickness of GaN layer is 10–20 nm and that of InGaN layer is 3 nm, respectively. Each layer grows on the wafer at an elevated temperature due to the heater coil under the susceptor. Atomic incorporation occurs from the adsorption layer into the crystal. The growth rate of the crystal can be assumed as the net difference between the adsorption and desorption rates.

A high quality of the growing material is normally promoted by the use of elevated temperatures and pressures in the growth reactor. Under the growth condition of high temperature and high pressure, a high efficiency of indium incorporation becomes a challenging task. Elevated temperatures enhance strongly indium desorption, whereas high pressures may intensify the formation of indium particles in the gas phase due to higher partial pressure of gaseous indium.

Indium surface segregation and compositional fluctuation in InGaN/GaN MQW heterostructures have been studied to identify the mechanism of light emission from nitride-based blue or green LEDs [2–7]. In order to suppress the indium segregation near the InGaN/GaN interfaces during the growth of In-rich InGaN layer, a growth interruption method [2–4] has been introduced before GaN capping, and then the quality of In-rich InGaN layer was greatly improved. During the measurement of phase segregation in InGaN quantum wells, the fluctuations were found to be between 10 nm and 20 nm in size and up to 20% on either side of the average composition [5]. Numerical predictions proposed to find possible ways for improvement of the quantum well composition uniformity were discussed [6–8]. This numerical model was validated by comparing the theoretical predictions with the data on composition profiles in GaN/InGaN/AlGaN quantum well

Contributed by the Fluids Engineering Division of ASME for publication in the JOURNAL OF FLUIDS ENGINEERING. Manuscript received April 3, 2007; final manuscript received July 12, 2007; published online July 30, 2008. Assoc. Editor: Dennis Siginer. Paper presented at the 5th Joint ASME/JSME Fluids Engineering Conference, San Diego, CA, July 30–August 2, 2007.

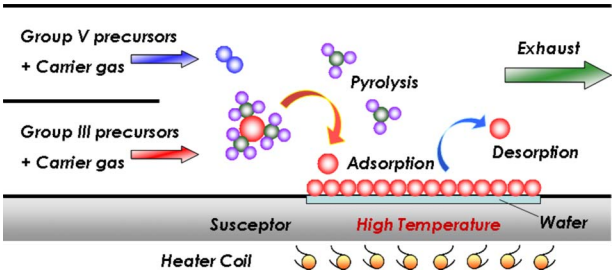

Fig. 1 Schematic of a classical MOVPE process for Group-III-nitride semiconductors

heterostructure. The comparison showed that the theoretical model reproduces quite well the lower interface of a quantum well.

In the present study, we have studied the characterization of three different commercial MOVPE reactors through both numerical and experimental approaches. Numerical simulations considering thermofluid dynamics, gas-phase chemical reactions, and chemical deposition on the surface have been validated by comparing with experimental data. Also, optimal speed of susceptor rotation was predicted for the temperature uniformity on the wafer due to the radio frequency (rf) induction heating.

Numerical Approach

Governing Equations. Computational fluid dynamics (CFD) simulations considering gas-phase chemical reactions and surface chemistry were carried out to establish the database on multiparametric dependency of indium incorporation and well thickness in a wide range of growth conditions. Governing equations are three-dimensional Navier–Stokes equations with vapor-phase chemical reactions:

$$\frac{D\rho}{Dt} + \rho\frac{\partial U_i}{\partial x_i} = 0 \tag{1}$$

$$\rho\frac{\partial U_j}{\partial t} + \rho U_i\frac{\partial U_j}{\partial x_i} = -\frac{\partial P}{\partial x_j} - \frac{\partial \tau_{ij}}{\partial x_i} + \rho g_j$$

$$\rho c_\mu\frac{\partial T}{\partial t} + \rho c_\mu U_i\frac{\partial T}{\partial x_i} = -P\frac{\partial U_i}{\partial x_i} + \lambda\frac{\partial^2 T}{\partial x_i^2} - \tau_{ij}\frac{\partial U_j}{\partial x_i} \tag{2}$$

where

$$\tau_{ij} = -\mu\left(\frac{\partial U_j}{\partial x_i} + \frac{\partial U_i}{\partial x_j}\right) + \frac{2}{3}\delta_{ij}\mu\frac{\partial U_k}{\partial x_k} \tag{3}$$

For an example of InGaN growth, trimethylindium (TMIn), triethylgallium (TEGa), and ammonia are used as the indium, gallium, and nitrogen precursors, respectively. The following vapor-phase chemical reactions are coupled with the above equations:

$$\mathrm{TMIn} \rightarrow \mathrm{MMIn} + 2\mathrm{CH_3} \tag{4}$$

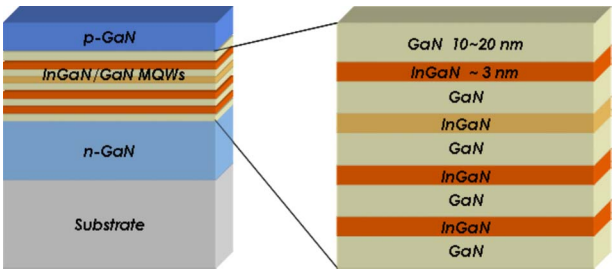

Fig. 2 Epitaxial structure of LED with InGaN/GaN MQWs

$$\mathrm{MMIn} \rightarrow \mathrm{In} + \mathrm{CH_3} \tag{5}$$

$$\mathrm{TEGa} + \mathrm{NH_3} \rightarrow \mathrm{TEGaNH_3} \tag{6}$$

$$\mathrm{TEGaNH_3} \rightarrow \mathrm{TEGa} + \mathrm{NH_3} \tag{7}$$

$$\mathrm{TMIn} + \mathrm{NH_3} \leftrightarrow \mathrm{TMInNH_3} \tag{8}$$

$$\mathrm{TEGa} \rightarrow \mathrm{Ga} + 3\mathrm{C_2H_5} \tag{9}$$

where the reaction constants of Eqs. (4)–(9) were determined by experimental measurements [7] and quantum mechanics calculations based on variational transition state theory [9,10]. The governing equations coupled with vapor-phase chemical reactions were solved with a finite volume method using a commercial flow solver well known as CFD-ACE+ [11]. For spatial discretization, a second-order upwind-difference scheme was adopted with limiters. For time integration for velocity solutions, the linear equation solver was the conjugate gradient squared (CGS) algorithm with preconditioning with 50 sweeps and a convergence criterion of 0.0001. The algebraic multigrid solver with 50 sweeps and a convergence criterion of 0.1 were also used for the other properties. This numerical approach can predict growth rates of GaN and InGaN layers as well as gallium and indium compositions in each layer by implementing the chemical vapor deposition (CVD) module [12] into the flow solver.

Modeling of Surface Chemistry. In the CVD module [12] released by STR Inc., the surface chemistry based on the quasithermodynamics approach was modified to consider the surface kinetics of Group-III nitrides [6]. A temperature dependent sticking/evaporation coefficient of molecular nitrogen on Group-III-nitride surfaces was implemented into the quasiequilibrium model of the molecular beam epitaxy (MBE) growth process. The values of the sticking coefficients were extracted from independent experimental data on Langmuir evaporation of binary nitrides in vacuum. The adsorption/desorption process can be described by using the Hertz–Knudsen equations that the net adsorption rate of the ith species at the surface can be expressed as

$$J_i = \alpha_i\beta_i(p_i - p_i^0) \tag{10}$$

where α_i is the sticking/evaporation coefficient accounting for kinetic limitations in the adsorption/desorption process, $\beta_i = (2\pi m_i kT)^{-1/2}$ is the Hertz–Knudsen factor for the ith species, p_i is the partial pressure of the ith species, near the growing surface, and p_i^0 is the equilibrium partial pressure of the ith species, which corresponds to the saturated vapor pressure of the species over its solid phase. The adsorption/desorption kinetics of ammonia and nitrogen on/from the surface of growing crystal can be considered by introducing the sticking coefficients of these species into the model. Regarding the interaction of nitrogen with the surfaces of Group-III nitrides, the nitrogen sticking coefficients were extracted from the independent experiments and evaluated as a function of temperature [13]. The approximate value of the ammonia sticking coefficient of 0.04 was measured in Ref. [14]. The sticking coefficients of all the other species are given by unity in the present study.

For modeling of InGaN growth at the surface, the experimental data were taken from Ref. [7] and the following independent heterogeneous reactions are considered as follows:

$$\mathrm{TEGa}(g) + \mathrm{NH_3}(g) = \mathrm{GaN}(s) + 3\mathrm{C_2H_5}(g) + 1.5\mathrm{H_2}(g) \tag{11}$$

$$\mathrm{TMIn}(g) + \mathrm{NH_3}(g) = \mathrm{InN}(s) + 3\mathrm{CH_4}(g) \tag{12}$$

$$2\mathrm{GaN}(s) = 2\mathrm{Ga}(g) + \mathrm{N_2}(g) \tag{13}$$

$$2\mathrm{InN}(s) = 2\mathrm{In}(g) + \mathrm{N_2}(g) \tag{14}$$

$$2\mathrm{Ga}(g) + \mathrm{H_2}(g) = 2\mathrm{GaH}(g) \tag{15}$$

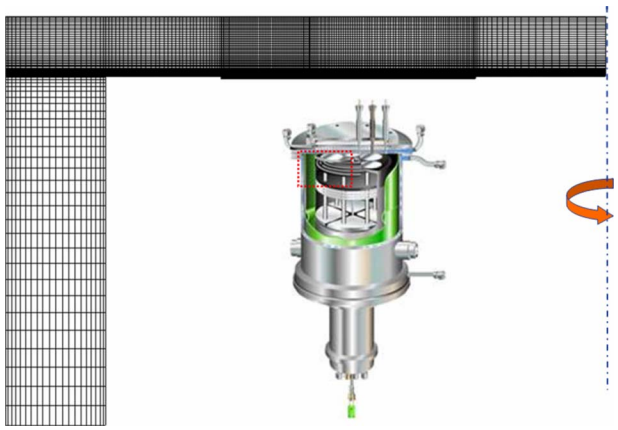

Fig. 3 Two-dimensional axisymmetric modeling of a vertical MOVPE reactor (Thomas Swan CCS reactor, 6×2 in. wafers)

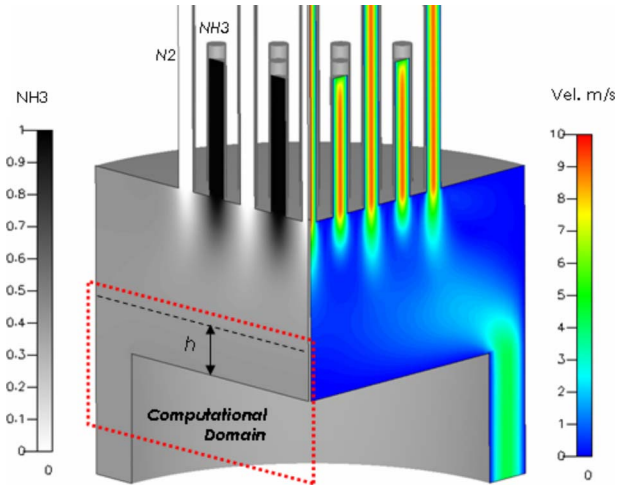

Fig. 4 Three-dimensional simulation for prediction of mixing layer thickness of ammonia (black) and nitrogen (white)

$$2\mathrm{In}(g) + \mathrm{H}_2(g) = 2\mathrm{InH}(g) \tag{16}$$

$$2\mathrm{NH}_3(g) = \mathrm{N}_2(g) + 3\mathrm{H}_2(g) \tag{17}$$

More detailed information on the basic principle and assumptions of the surface chemistry modeling for Group-III nitrides can be found in previous studies [6,12].

Experimental Approach

Various growth experiments have been performed in commercial MOVPE reactors to understand the growth mechanism of Group-III nitrides. After heating the rf coil up to the desired growth temperature, TMIn, trimethylgallium (TMGa), and TEGa as group-III precursors, along with 100% ammonia as Group-V sources, were introduced into the reactor to grow the InGaN/GaN MQWs following *n*-GaN layer on 0.2 deg tilted sapphire (0001) substrates. The temperature of substrate holder, so-called susceptor, was monitored and controlled using a near-infrared pyrometer.

For determination of growth rate and strain, the high resolution x-ray diffractometry (HXRD) was used. Also, indium compositions of InGaN layers were determined by photoluminescence (PL) spectroscopy using an excitation beam of a 266 nm frequency tripled Nd:YAG laser.

Results and Discussion

Vertical-Type Reactor. A commercial MOVPE (i.e., Thomas Swan's close coupled showerhead, six wafers by 2 in. diameter) reactor was modeled and then simulated under a typical growth condition for In-rich InGaN/GaN MQW heterostructures. Trimethyl compounds of indium and gallium (i.e., TMIn and TMGa) are used as metal organic precursors and chemically react with 100% ammonia at a reactor pressure of 300 Torr and a growth temperature of 1003 K.

For computational efficiency, the reactor was modeled as two dimensional axisymmetric and the total grid size was 10,773 nodes, as shown in Fig. 3. The maximum normalized residual for convergence criterion was less than 10^{-4} in about 1000 iterations

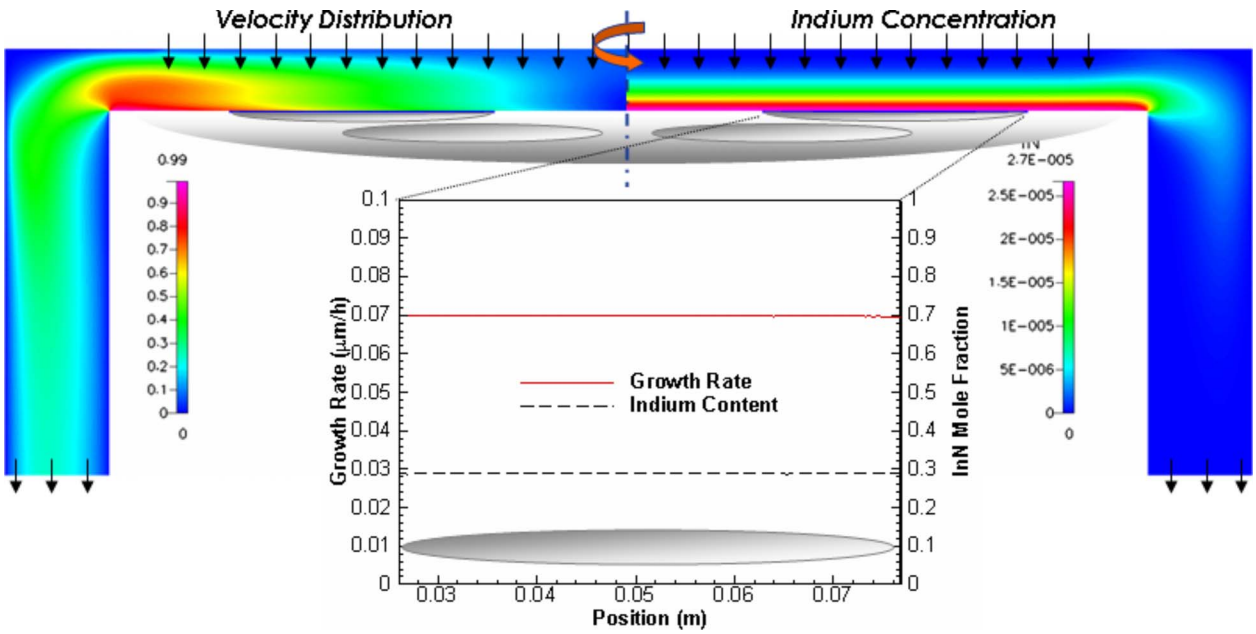

Fig. 5 Contours of velocity magnitude and gas-phase indium distribution (top) and growth rate and indium content on a wafer surface (bottom)

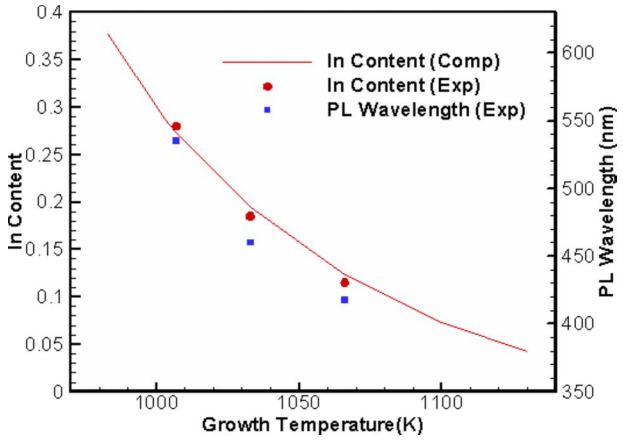

Fig. 6 Comparison of computed and experimental data in indium content and PL wavelength in a wide range of growth temperature

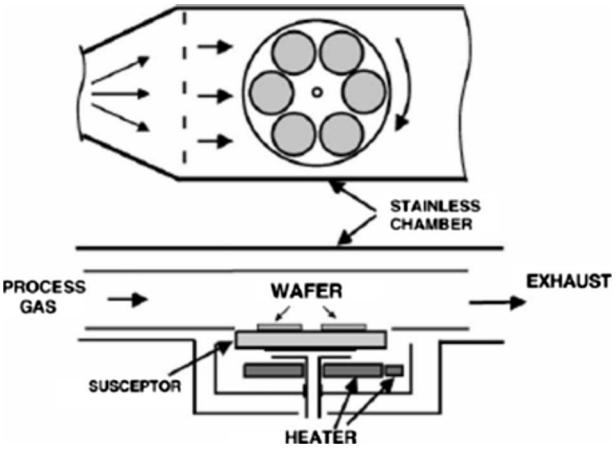

Fig. 7 Schematic drawing of horizontal multiwafer MOVPE reactor (Nippon Sanso SR6000, Tokunaga et al. [15])

and the elapsed time was 5500 s on an HP Workstation xw8200 with 3.6 GH CPU. Ammonia and carrier gases (nitrogen and/or hydrogen) are introduced into the reactor through numerous separate inlet holes in order to avoid prereactions outside the reactor chamber. It costs a lot of time and effort to numerically model the whole system including those inlet holes. Thus, a local computational domain was considered as defined in the diamond-shaped box since we noticed that the mixing layers of ammonia and nitrogen are fully developed not far from their inlets, as simulated in Fig. 4. For a simple test to predict the approximate thickness of mixing layers, only two dozens of inlet holes were modeled without considering susceptor rotation. Actually the mixing layer thickness was quite smaller than the height of the reactor chamber.

However, instead of full modeling of inlet pipes, we have included the surface chemistry and susceptor rotation for final results, as shown in Fig. 5. A uniform layer of high-concentration vapor-phase indium is observed on the high-temperature susceptor. Because of the susceptor rotation, the magnitude of velocity increases along with the susceptor radius. It was found that the susceptor rotation of 100 rpm results in a higher uniformity of growth rate and indium composition on wafer. Predicted values of growth rate and indium composition are 1.17 nm/min and 28.8%, respectively. Compared to experimental measurements, simulation results give over 90% accuracy for the growth rate as well as the indium composition. For a wide range of growth temperature, computed results of indium composition show quite a good agreement with experimental data, as shown in Fig. 6. It was also noticed that (PL) wavelength shows a similar tendency with the indium content, which has been well proved in many experimental measurements.

Horizontal-Type Reactor. Another commercial MOVPE system (SR6000, 6×2 in. wafers) has been developed by Nippon Sanso Co. and it has a horizontal-type reactor, as depicted in Fig. 7. This reactor was modeled with approximately 82,200 grid cells, as shown in Fig. 8. Since this reactor was not available in our affiliate, we simulated this reactor and then compared the computed results with the experimental measurements taken for Ref. [15]. They showed that uniformity and reproducibility of doping and film thickness were typically better than $\pm2\%$ across a full 2 in. wafer. PL peak wavelength uniformity was better than 450 ± 7 nm across a full 2 in. wafer. As already observed in Fig. 6, indium content shows quite a similarity with PL peak wavelength. The PL peak wavelength can be expressed as a function of

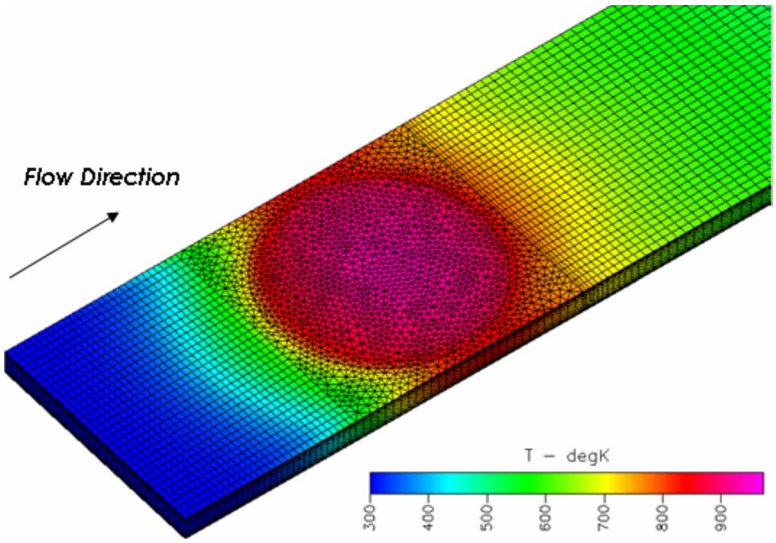

Fig. 8 Three-dimensional modeling of horizontal MOVPE reactor (Nippon Sanso SR6000) and its temperature distribution during InGaN growth

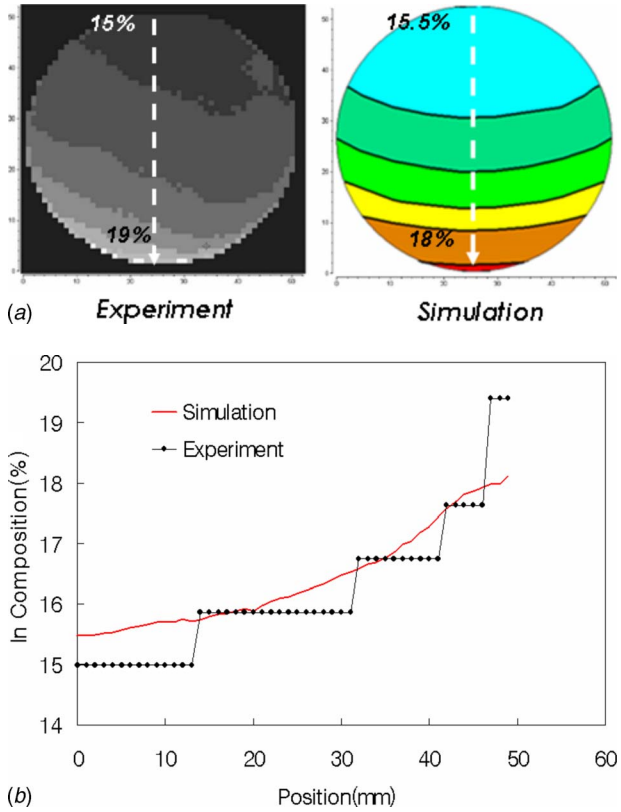

Fig. 9 Comparison of experimental and computed indium distributions on a 2 in. full wafer; (*a*) contour lines of indium composition with the maximum and minimum values (left: experiment; right: simulation); (*b*) indium composition along a centerline

thickness and indium composition of InGaN layer. Gain peak wavelength simulation showed the relationship as

$$\lambda_{PL}(\text{nm}) = 261.7 + 680.0X_{In} + 23.0t_{layer}(\text{nm}) \quad (18)$$

where λ_{PL} is the peak wavelength, X_{In} is the indium composition, and t_{layer} is the thickness of the InGaN layer.

The PL mapping result was converted into indium composition contour lines, and then compared, as shown in Fig. 9. Computed indium distribution on a 2 in. full wafer shows a good agreement with converted experimental data. Simulation shows the minimum maximum range of 15.5–18% indium composition, whereas experimental measurement shows approximately 15–19% in Fig. 9(*a*). For the indium composition along the centerline, the simulation shows a good agreement with experimental data, as shown in Fig. 9(*b*).

Planetary Reactor. In addition, a large-scaled commercial MOVPE (AIXTRON's planetary multiwafer, 2 in.×11 wafers)

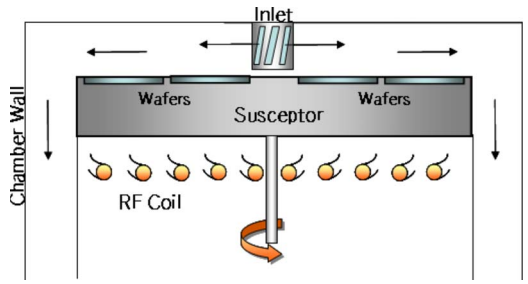

Fig. 10 Schematic drawing of a planetary MOCVD reactor

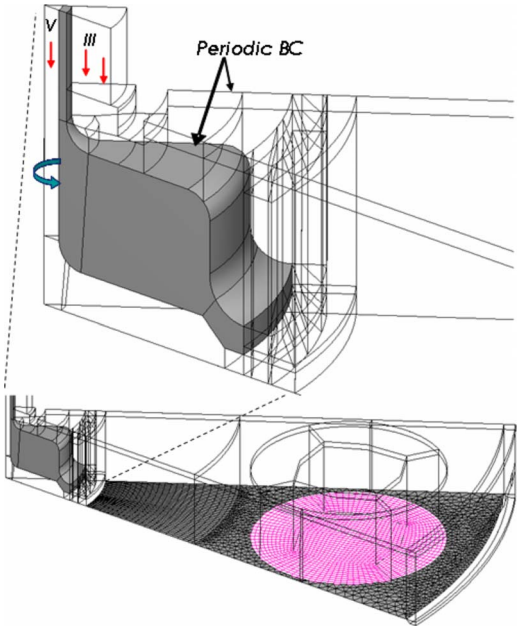

Fig. 11 Three-dimensional modeling for one-eleventh of the whole reactor with centrifugal inlet nozzles (AIXTRON planetary reactor, 11×2 in.)

system was also simulated to investigate the high-temperature flow field in the planetary reactor, as depicted in Fig. 10. The growth temperature for the InGaN layer was given by 750°C and the reactor pressure was maintained as 300 Torr. Independent of the main susceptor rotation, each wafer holder was designed to self-rotate by 50 rpm in order to improve the uniformity of growth rate and composition distribution at high-temperature conditions. Group-V precursors such as 100% ammonia and the trimethyl compounds of gallium and indium are introduced into the reactor chamber through the two dozens of centrifugal inlet nozzles. For

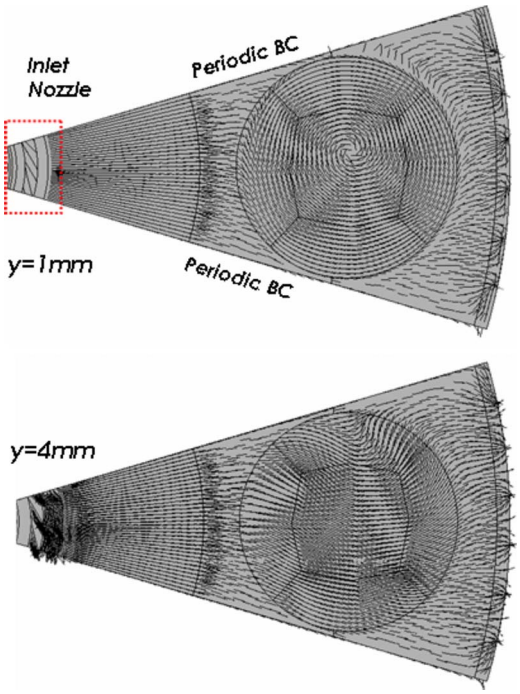

Fig. 12 Velocity vectors on two planes at 1 mm and 4 mm above the susceptor with a wafer rotation of 50 rpm

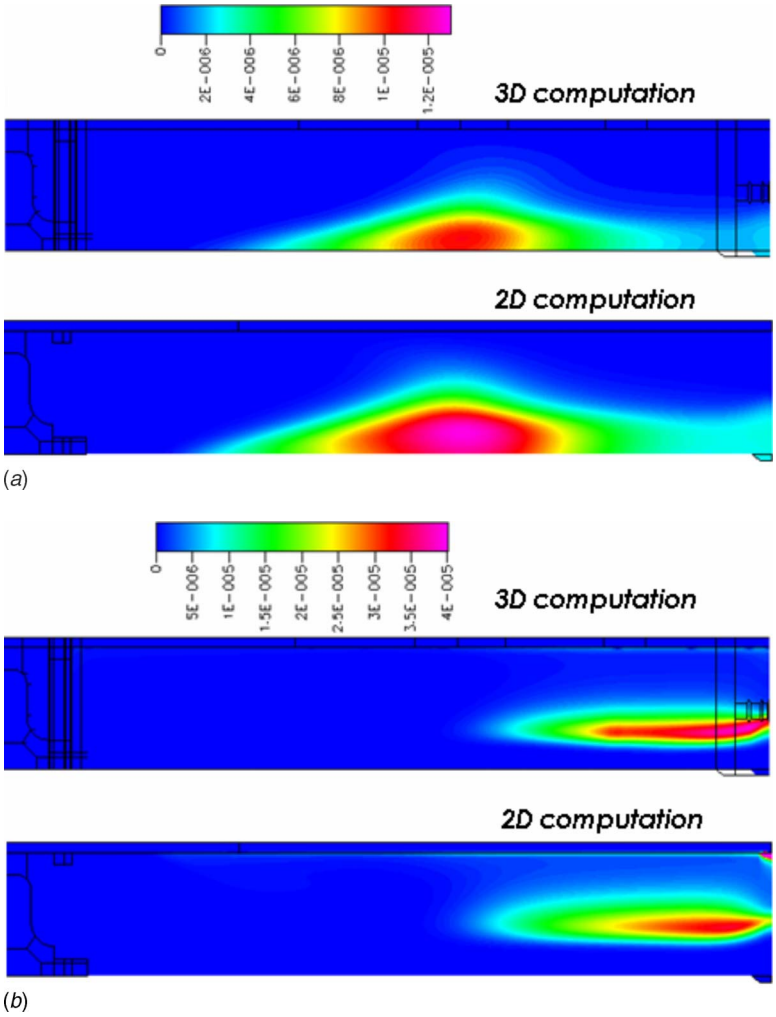

Fig. 13 Comparison of two- and three-dimensional flow fields with and without wafer orientation; (*a*) contours of indium molar fraction; (*b*) contours of particle density of indium clusters

computational efficiency, only one-eleventh of the entire domain with total 22,000 grid cells was modeled, as shown in Fig. 11. Rotating wall boundary conditions were imposed onto the wafer surfaces and periodic boundary conditions were given to both sides of the computational domain.

Figure 12 shows velocity vectors on both planes above the susceptor at 1 mm and 4 mm, respectively. Swirling vectors are also observed on the self-rotating wafer. The distributions of the indium molar fraction and particle density were obtained from both two- and three-dimensional approximations and then compared for the central cross section of the reactor. Three-dimensional modeling predicts somewhat lower indium concentration and higher particle density of indium clusters, as shown in Fig. 13. These differences attribute to self-rotation of each wafer in three-dimensional simulations. Because of the self-rotational motion, the flow residence time becomes longer, which promotes particle formation.

RF Induction Heating. Uniform temperature distribution around the susceptor is crucial in obtaining homogeneous MQWs with high indium composition. For a precise thermal control, heating methods using rf power have been widely adopted in MOVPE system. Thus, we have modeled and simulated inductance heating problems in a rf heater unit for 2 in. $\times$ six-wafer MOVPE reactor, as shown in Fig. 14.

Three-dimensional thermal flows in the same magnetic field were simulated for two cases with susceptor rotational speeds of 0 rpm and 5 rpm, as shown in Figs. 14(*a*) and 14(*b*), respectively. Operation gas was assumed nitrogen of 75 slm, magnetic field source was generated by 30 kHz ac in the copper coil, and current density is 1.75×10^7 A/m^2. For the stationary susceptor (i.e., no susceptor rotation), the front region has the lower-temperature distribution than the rear since the inlet flow of precursor gases cools down the front, as observed in Fig. 14(*a*). Along with the susceptor rotation, the difference between the maximum and minimum temperatures on the susceptor decreases, as shown in Fig. 15. It is found that the temperature uniformity within 3 °C standard deviation on all the wafers can be guaranteed with the minimal rotational speed of 5 rpm or more.

Conclusion

Both numerical and experimental approaches have been carried out to characterize the MOVPE growth of InGaN/GaN MQW. Typical features of three different MOVPE reactors were simulated using CFD with vapor-phase chemical reactions and surface deposition. Those CFD simulations have been verified by comparing with experimental data for growth rate and indium composition of the InGaN layer in a wide range of growth temperature. Some rf induction heating simulations were also conducted to predict a minimal susceptor rotating speed of 5 rpm for uniform temperature distribution. The present approach combining numeri-

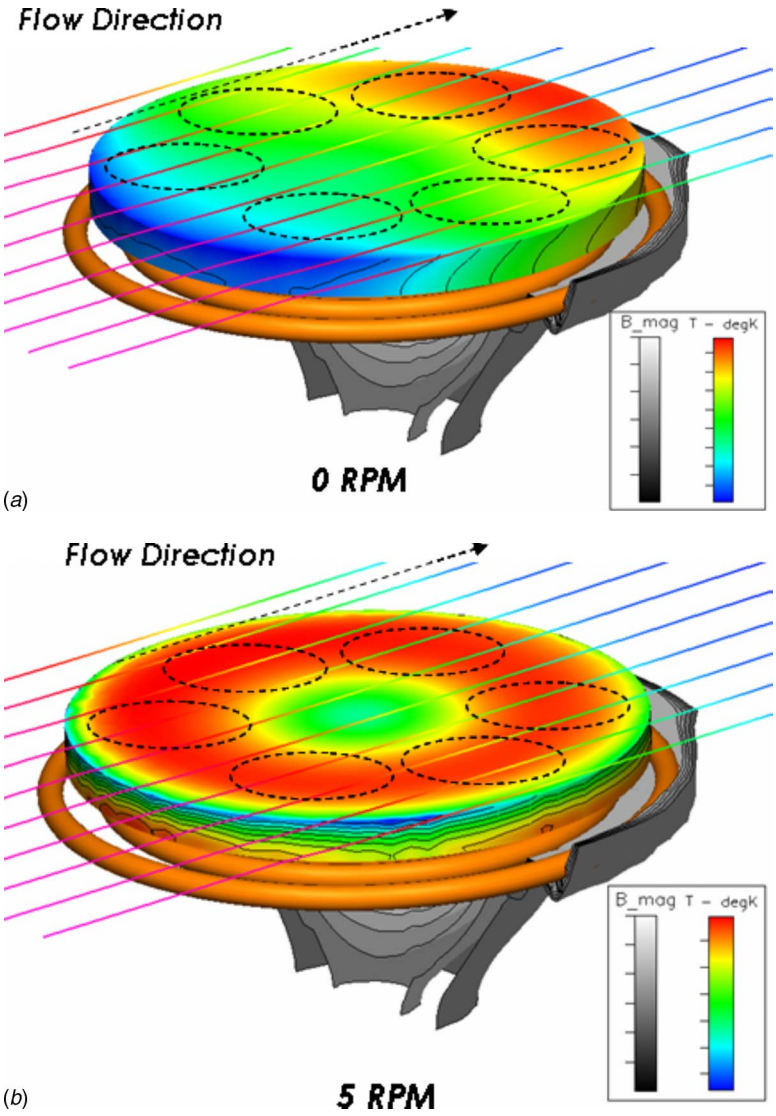

Fig. 14 Temperature (color-scale) and magnetic (gray-scale) fields of a rf heater with two different susceptor rotating speeds

cal simulation based on CFD and experimental measurement has been successfully applied to the development of in-house metal organic chemical vapor deposition (MOCVD) system as well as the performance enhancement of existing commercial MOCVD reactors.

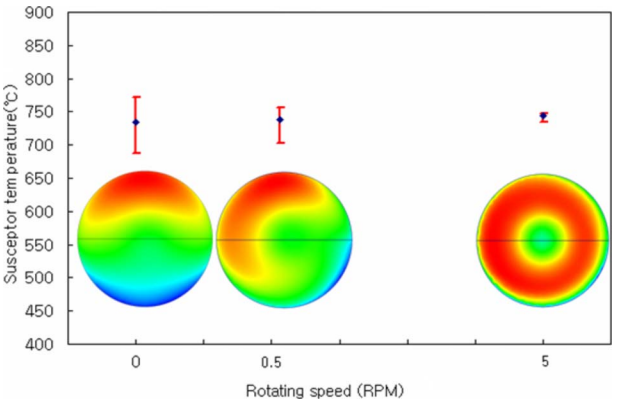

Fig. 15 Temperature distribution on the susceptor with respect to rotating speed

Acknowledgment

The authors would like to thank Dr. Roman A. Talalaev and Eugene V. Yakovlev at Soft-Impact Ltd., Dr. Yuri Makarov at STR Inc., and Dr. Lada V. Yashina at Moscow State University for their technical support and discussion.

Nomenclature

c_μ = specific heat
DMIn = dimethylindium
k = Boltzmann constant
m = mass of molecule, kg
MMIn = monomethylindium
p = pressure, N/m^2
t = time,
T = temperature, K
U, V, W = velocity vectors, m/s
x, y, z = spatial coordinates, m

μ = fluid viscosity, kg/m s
ρ = density, kg/m^3
τ = stress tensors

References

[1] Nakamura, S., and Fasol, G., 1997, *The Blue Laser Diode*, Springer, Berlin.
[2] Moon, Y.-T., Kim, D.-J., Song, K.-M., Choi, C.-J., Han, S.-H., Seong, T.-Y., and Park, S.-J., 2001, "Effects of Thermal and Hydrogen Treatment on Indium Segregation in InGaN/GaN Multiple Quantum Wells," J. Appl. Phys., **89**(11), pp. 6514–6518.
[3] Cho, H. K., Lee, J. Y., Sharma, N., Humphreys, J., Yang, G. M., and Kim, C. S., 2001, "Structural and Optical Characteristics of InGaN/GaN Multiple Quantum Wells With Different Growth Interruption," Phys. Status Solidi B, **228**(1), pp. 165–168.
[4] Kwon, S.-Y., Kim, H. J., Na, H., Kim, Y.-W., Seo, H.-C., Kim, H. J., Shin, Y., Yoon, E., and Park, Y., 2006, "In-Rich InGaN/GaN Quantum Wells Grown by Metal-Organic Chemical Vapor Deposition," J. Appl. Phys., **99**, p. 044906.
[5] Duxbury, N., Bangert, U., Dawson, P., Thrush, E. J., Van der Stricht, W., Jacobs, K., and Moerman, I., 2000, "Indium Segregation in InGaN Quantum-Well Structures," Appl. Phys. Lett., **76**(12), pp. 1600–1602.
[6] Karpov, S. Yu., Prokofyev, V. G., Yakovlev, E. V., Talalaev, R. A., and Makarov, Yu. N., 1999, "Novel Approach to Simulation of Group-III Nitirdes Growth by MOVPE," MRS Internet J. Nitride Semicond. Res., **4**(4), pp. 1–7.
[7] Talalaev, R. A., Yakovlev, E. V., Karpov, S. Yu., Makarov, Yu. N., Schoen, O., Heuken, M., Strauch, G., and Juergensen, H., 1999, "Modeling of InGaN MOVPE in AIX 200 Reactor and AIX 2000 HT Planetary Reactor," MRS Internet J. Nitride Semicond. Res., **4**(5), pp. 1–5.
[8] Karpov, S. Yu., Talalaev, R. A., Evstratov, I. Y., and Makarov, Yu. N., 2002, "Indium Segregation Kinetics in MOVPE of InGaN-Based Heterostructures," Phys. Status Solidi A, **192**(2), pp. 417–423.
[9] Schmid, R., and Basting, D., 2005, "Gas Phase Chemistry in Gallium Nitride CVD: Theoretical Determination of the Arrhenius Parameters for the First Ga-C Bond Homolysis of Trimethylgallium," J. Phys. Chem. A, **109**(11), pp. 2623–2630.
[10] Kim, C. S., Shim, J., Hong, J., Moon, W. H., Ji, S.-Y., Yoon, Y. J., Kim, B. J., Park, S.-E., Han, J. W., and Lee, W. S., 2007, "Precise Composition Control of InGaN/GaN Multi Quantum Wells in Metal Organic Vapor Phase Epitaxy," SAMSUNG Journal of Innovative Technology, **3**(1), pp. 23–32.
[11] 2004, CFD-ACE+ V2004 Module Manual, Vol. 2, pp. 112–140.
[12] Karpov, S. Yu., 2003, "Advances in the Modeling of MOVPE Processes," J. Cryst. Growth, **248**, pp. 1–7.
[13] Averyanova, M. V., Przhevalsky, I. N., Karpov, S. Yu., Makarov, Yu. N., Ramm, M. S., and Talalaev, R. A., 1997, "Analysis of Vaporization Kinetics of Group-III Nitrides," Mater. Sci. Eng., B, **43**, pp. 167–171.
[14] Mesrine, M., Grandjean, N., and Massies, J., 1998, "Efficiency of NH3 as Nitrogen Source for GaN Molecular Beam Epitaxy," Appl. Phys. Lett., **72**(3), pp. 350–352.
[15] Tokunaga, H., Tan, H., Inaishi, Y., Arai, T., Yamaguchi, A., and Hidaka, J., 2000, "Performance of Multiwafer Reactor GaN MOCVD System," J. Cryst. Growth, **221**, pp. 616–621.